OPTICAL REVIEW Vol. 16, No. 4 (2009) 426–431

Tomographic Imaging of Incipient Dental-Caries Using Optical Coherence Tomography and Comparison with Various Modalities

Jihoon NA, Jae Ho BAEK[1], Seon Young RYU, Changsu LEE[2], and Byeong Ha LEE

Department of Information and Communications, Gwangju Institute of Science and Technology (GIST), 261 Cheomdan-gwagiro, Buk-gu, Gwangju 500-712, Korea
[1]*Department of Orthodontics, Division of Dentistry, Ulsan University Hospital, 290-3 Jeonha-dong, Dong-gu, Ulsan 682-714, Korea*
[2]*Department of Electronic Engineering, The University of Suwon, Bongdam, Hwaseong, Gyeonggi 445-743, Korea*

(Received December 27, 2008; Accepted March 24, 2009)

We present the optical coherence tomography (OCT) made to investigate the early dental caries in human teeth and compare its results with those taken by conventional imaging modalities including light illuminating examination (LIE), digital intra-oral radiography (DIOR), and electron probe micro analyzer (EPMA). Morphological features and caries-involved areas of the dental structure were mainly investigated by LIE, DIOR, and OCT to study the infection of the caries lesion in pits and fissures. The biochemical information acquired with EPMA and the morphological features taken with OCT in the early stage of caries were compared and analyzed to present an objective and practical index for the degree of caries. The experimental results allow us to conclude that OCT could be used to provide quantitative analysis of caries based on the reflectivity difference in the specimen. © 2009 The Optical Society of Japan

Keywords: optical coherence tomography, biomedical imaging, medical optics instrumentation, dental decay, early caries

1. Introduction

Dental caries is a microbial disease of the calcified tissue of a tooth, which is well characterized by demineralization of the inorganic portion and destruction of the organic substance of the tooth.[1)] This microbiological transformation results in loss of tooth substances such as calcium and phosphate.[2)] Even in well-developed countries, dental caries is one of the most prevalent chronic diseases. Like other diseases early detection is important for the treatment of dental caries. Although there are various diagnostic aids for such detection, including radiography and specialized dye, some problems still exist. Because there are various stages in the progress of dental caries, especially in its early stage, it is not easy to differentiate the caries properly. When the caries is in its early stage, the infected tooth could be reinforced with tooth brushing and/or re-hardened with fluoride application. However, the severely progressed part of the infected tooth must be mechanically removed permanently and replaced with other materials such as amalgam, composite resin, or gold. Therefore, diagnosis of the caries in its early stage is very important.

However, conventional diagnostic methods are not effective enough to differentiate the early caries in most cases, therefore unnecessary irreversible treatment might be made occasionally. Researches[3–6)] have shown that re-hardening of the tooth surface, which had previously been softened by exposure to acid solutions, could be achieved by exposing the softened tooth in a calcium phosphate solution. The re-hardening can be accelerated by treating it with a 1.0 ppm fluoride solution. It is common sense that even minute variation in the incipient caries can save or conserve more tooth materials and prevent unnecessary fearful dental treatments. Therefore, it is necessary to develop a new diagnostic aid that can differentiate even minute changes in dental caries with a real time and non-invasive manner.

In this paper, we employ four different imaging modalities including eye inspection (EI), digital intra-oral radiography (DIOR),[7)] light illuminating examination (LIE),[8)] and electron probe micro analyzer (EPMA)[9)] to study human teeth infected by caries lesions on enamel and dentin *in vitro*, and compare them with optical coherence tomography (OCT).[10)] Preliminary OCT imaging on a human tooth is firstly presented and the comparison with other conventional imaging modalities follows. The biochemical changes acquired with EPMA and the morphological features taken with OCT are compared and analyzed primarily to present a practical index for translating the degree of the dental caries in its early stage.

2. Materials and Methods

2.1 Imaging modalities

The easiest and fastest way to examine dental caries is EI. This is usually done with naked eyes but it includes taking photographs for contrast enhancement and/or saving it as data. However, with EI it is difficult to decide whether the caries is in early stage or not, thus an unnecessary dental treatment might be performed.

DIOR is one of the most popular diagnostic imaging systems in dentistry.[7)] However, this modality can be used only to the caries that has progressed to a certain degree. After the eye inspection on a large scale, DIOR is generally employed to confirm the observation. If the caries lesion is detected by DIOR, a series of subsequent dental treatments including irreversible mechanical removal of the infected area is generally accompanied. The digital radiographic aid

used in this experiment (Planmeca Intra, Planmeca Oy) had a 38 μm pixel size and a 16 lp/mm resolution.

LIE with a light curing unit is another convenient clinical method for detecting caries.[8] It is often used to present results of restoration or to find fine fracture lines within a tooth by visual inspection. We used a commercial light curing instrument (3M ESPE, Eliper Freelight 2) that had a light intensity of 1,000 mW/cm^2 and a wavelength range of 440–500 nm.

EPMA provides the distribution of chemical compositions (mainly calcium and phosphate) in a hard tissue.[9] It irradiates a focused electron beam having typically 5–60 kV energy on a specimen, and collects the X-ray photons emitted at various elemental chemical species by the electron beam. The chemical composition of the sample under test is identified by the wavelength spectrum of the emitted X-ray photons. EPMA is a fully qualitative and also quantitative method suitable for chemical composition analysis with a ppm sensitivity level. The EPMA unit used for this experiment (Cameca SX100) had a ~20 μm electron beam size.

OCT is a real time, non-invasive, and high resolution diagnostic imaging modality, which has been widely used to produce cross-sectional or volumetric images of biological tissues.[10] As an imaging modality, owing to its high axial and transversal resolutions, OCT is expected to greatly improve the clinical management of malignant diseases. Basically, the transverse resolution of an OCT system is determined by the focusing optics, while the spectral bandwidth of the light source determines its axial resolution. The focusing lens having a higher numerical aperture gives the better resolution in the transverse direction, and the light source having a wider spectral bandwidth gives the higher resolution in the axial direction. The performance of an OCT system is mainly evaluated by its axial resolution and the scanning speed.[11] Recently, Fourier domain detection techniques using frequency swept lasers or spectrometers are very popular for real-time imaging.[12–14]

Previously, Colston *et al.*[15] has firstly employed OCT for *in vitro* and *in vivo* imaging of dental structures. Feldchtein *et al.*[16] has reported the imaging of hard and soft tissues containing oral mucosa, caries of a tooth, and dental restorative procedures. Amaechi *et al.*[17] measured the reflectivity variation, induced by demineralization, for quantitatively assessing the dental caries lesion. Wang *et al.*[18] has applied polarization-sensitive OCT (PS-OCT) for characterizing dentin and enamel, and Fried *et al.*[19] has also shown the images of caries lesions and the lesion progression with PS-OCT. Brandenburg *et al.*[20] have imaged demineralized tissues, caries lesions, restored teeth, and oral mucosa. Recently, Kyotoku and Gomes[21] reported an *in vitro* study analyzing the fracture propagation in a fiber reinforced composite material by spectral domain OCT (SD-OCT).

Although previous works have shown very good OCT results involving caries lesions, the comparison with various imaging modalities has not been demonstrated. Most of the works have dealt with OCT itself to analyze caries lesions. However, detecting the stage of the caries lesion is very important, especially its incipient stage, and comparison with other modalities is also necessary to evaluate the OCT performance and to investigate how the lesion progresses.

In this study, we focus on the feasibility of detecting the changes in the microstructure of human tissues, especially dental decay in its incipient stage from a diagnostic point of view. Many dental diseases, related to oral cavities, are usually originated from a change in tissue structures. Typical examples are caries and non-caries lesions in teeth, periodontal diseases, and oral tumors. The ability to perform high-resolution diagnostic imaging is therefore required to detect and treat these diseases. Radiography displays a spatial resolution up to 16.5 lp/mm under an ideal environment and *in vitro*.[22,23] However, OCT is expected to overcome the limitations of other modalities and give more precise clinical features such as location of the soft tissue attachment, morphological change, tooth decay, and structural maintenance of dental restorations. Therefore, we measure the OCT images of human teeth and compare them with those obtained with other conventional modalities.

2.2 *Samples preparation*

An extracted human tooth (premolar, 32-year-old male) was used to examine the early dental caries with various modalities including OCT. The sample was chosen for studying the incipient caries progressing only in pit and fissure to analyze the degree of destruction in the enamel region. The sample was cut by a diamond saw to reveal the infected area, and then EI, LIE, and DIOR were employed. For the EPMA test, the sample surface was carefully polished with diamond and silicone paper discs in sequence. Then, the sample was fixed in a silicone mold and coated with gold. The silicone mold protected the small sample and held the sample surface parallel to assure the best result of the EPMA test. For the OCT imaging, sample scanning was made from the side of the sample. We have tried to make OCT scan very near to the cutting region of the sample.

3. Experimental Setup for OCT Imaging

The time-domain OCT system implemented with a fiber-based Michelson interferometer was used for experiments. Figure 1 shows a schematic of the experimental setup. A broadband light source having an output power of 4 mW, center wavelength of $\lambda_c = 1310$ nm, and bandwidth of $\Delta\lambda = 58$ nm was utilized. The axial resolution of the system was measured to be 14 μm in air, which was in good agreement with the theoretical one of 13 μm.[10] The rapid-scanning optical delay line (RSOD) was placed in the reference arm of the interferometer for the axial scanning.[24] The RSOD was implemented with a low cost galvanometer operating at a 200 Hz repetition rate. A small angular excursion of 4° in the galvo-mirror was set to obtain a group delay scan range of ~2.5 mm. The corresponding carrier frequency of the interferogram was measured to be 166 kHz.

The light back-reflected from the reference mirror and the one back-scattered from the sample were recombined at the coupler and subsequently delivered to the detector (D1 and

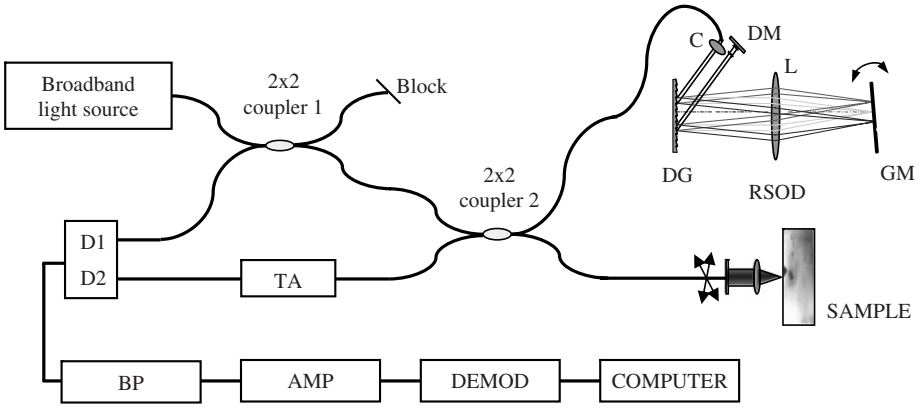

Fig. 1. (Color online) Schematic of a fiber-based time domain OCT system. RSOD, rapid-scanning optical delay line; C, collimator; DM, double pass mirror; DG, diffraction grating; L, lens; GM, galvano mirror; TA, tunable attenuator; D1, D2, InGaAs photodiodes; BP, band-pass filter; AMP, amplifier; DEMOD; demodulator.

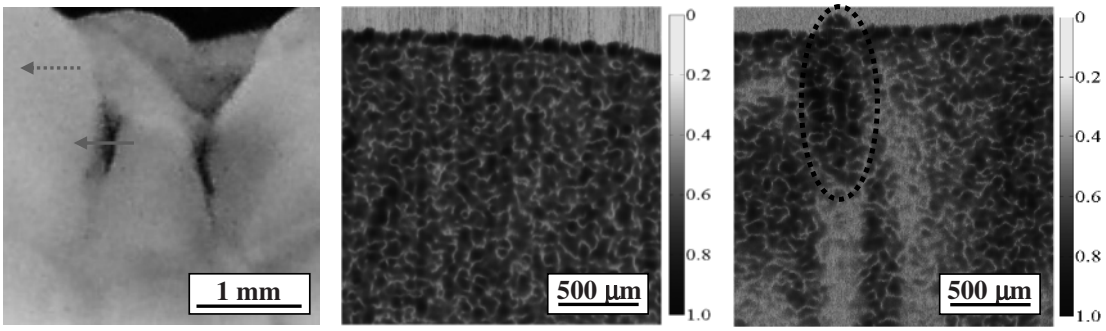

Fig. 2. (Color online) Photograph (a) and OCT images of normal region (b) and caries region (c). The dotted and solid arrows indicate the scanning directions of the non-caries and the caries regions, respectively.

D2). To enhance the interference signal contrast, a tunable attenuator was utilized, and a dual-balanced detector (New Focus 1817) was employed to minimize DC and autocorrelation signals.[25] The balanced detector is well known and widely employed in a standard OCT system. Coupler 1 in the figure was employed to get the signals for the balanced detector.

As is well known, OCT is operated with the principle that optical interference happens only when the optical path length difference between two arms of an interferometer is less than the coherence length of the light source. While scanning the reference arm, the interference signal is detected by an intensity detector such as a photodiode and then processed with a band-pass filter to minimize the noise. To extract the axial or depth information of the sample, the signal is electronically demodulated. The extracted envelope signal is then digitized and used to construct a tomographic line scan (A-scan) image of the sample with a personal computer. A cross-sectional image is then obtained by transversely scanning the beam across the sample (B-scan). A total number of 1,000 axial A-scans were made to obtain a single two-dimensional OCT image. Each A-scan analog signal was sampled at 2,048 points and converted to digital signals with 12 bits.

4. Results and Discussion

4.1 Preliminary study

In this section, we only discuss the difference of OCT images for the normal and abnormal enamel regions. A human tooth consists of three major components: enamel, dentin, and pulp. Enamel is porous and composed of rod-like elements called the enamel rods, approximately 4 μm wide and 8 μm long depending on location. Dentin is composed of a mixture of collagenous proteins, which forms a multiplicity of fluid and dentinal tubules. For the preliminary study of OCT, the enamel region of an extracted human tooth (molar, male) was imaged with the OCT system of Fig. 1.

Figure 2(a) shows the photograph of the cut surface of the tooth that has early caries. Along the dotted arrow a normal or control OCT image was taken and shown in Fig. 2(b). Along the solid arrow the OCT image on an early caries was taken and shown with Fig. 2(c). The worm-like texture in the OCT images represented the dental tubes in the enamel. However, because of irregular speckle patterns and specula reflections in the specimen, detailed structure information was not well identified. The stage of the caries in Fig. 2(c) was an incipient case even though it was distinguished by

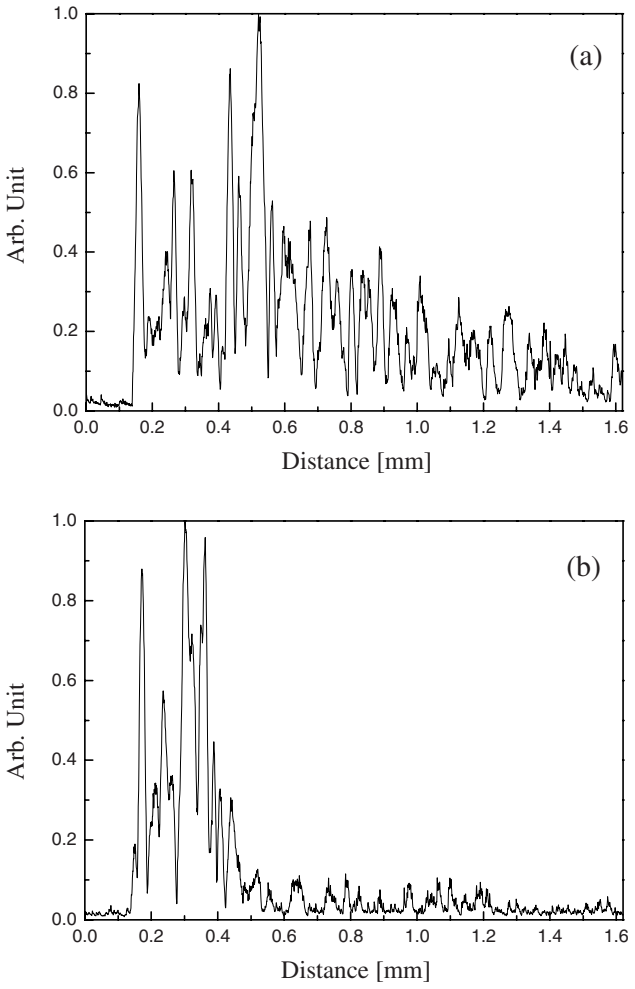

Fig. 3. The axial scanning (A-scan) signals of Fig. 2; one was for the normal enamel region (a) and the other for the region of caries lesion (b). The incident light penetrated deeper in the normal region.

eye inspection. As marked with a dotted circle in Fig. 2(c) and presented with a scale bar, the infected area gave a strong OCT signal. However, due to the strong light reflection or scattering at the caries, below the caries region we could not see appreciable OCT signals. This explains the white part (no OCT signal region) located just below the dotted circle of Fig. 2(c).

To see the detail, the depth profile along an axial A-scan line was expatiated in Fig. 3; one A-line per each OCT image of Fig. 2. At the normal enamel region, the OCT could image deeper than 1.6 mm as shown with Fig. 3(a); while, at the caries region, it could image only up to 0.5 mm from the surface as could be seen in Fig. 3(b). Based on these preliminary results, the OCT measurement is made with the sample prepared at §2.2 of this article, and the OCT image is compared with those obtained with conventional EI, DIOR, LIE, and EPMA, as follows.

4.2 Comparison with other imaging modalities

The sample tooth (premolar, 32-year-old male) for this main experiment was prepared as explained in §2.2. Images of the tooth were successively taken with different imaging modalities and collectively shown in Fig. 4. The dotted ellipse in each figure indicates the region of incipient caries. Figure 4(a) is the image of EI, Fig. 4(b) is the one of DIOR, and Fig. 4(c) is the result of LIE. The results of EPMA measurements are Fig. 4(d) for the calcium concentration and Fig. 4(e) for the phosphate concentration. Finally, the OCT image of the same sample is shown with Fig. 4(f).

As mentioned, the EI of the sample Fig. 4(a) was made after dissecting the tooth with a diamond saw and disclosing the infected area. In this cross-sectional photograph view, we were able to identify the caries region because the color was changed at the infected region. However, the incipient caries was not observed before cutting the sample or using the whole tooth. In the image of DIOR, Fig. 4(b), we could not distinguish the caries region due to the resolution limit and/or the inherent weak sensitivity of X-ray to the incipient caries. DIOR is simple but harmful in general because of ionizing radiation to patients. Furthermore, it provides only overlapped images and has a resolution inadequate for examining early caries or catching micro-structural changes.

The image obtained with LIE could distinguish the caries region as shown in Fig. 4(c). However, it should be noted that the LIE measurement was made with the dissected sample as already mentioned with Fig. 4(a). With the whole tooth, thus the caries located inside, we could not distinguish the caries by LIE. In general, since the caries destroy the regular crystal-like structure of a tooth, the caries-involved area becomes darker, thus can be observed by EI and LIE in a proper condition. Even though LIE is very convenient and the measurement is made in a short time, it cannot distinguish the severity of caries and often confuses a normal pit or fissure with caries.

In the EPMA test, we analyzed two chemical elements (calcium, phosphate) to evaluate the minute change in the caries-involved area. Calcium and phosphate are known as the main inorganic materials that compose the enamel. In general, if the caries progresses, the amounts of calcium and phosphate at that specific area become decreased. The EPMA measurements showed that in the infected region the calcium concentration, Fig. 4(d), and the phosphate concentration, Fig. 4(e), were severely decreased. As can be seen with the color-scale bar, the loss of calcium was slightly worse than that of phosphate. The EPMA images are very clear qualitatively and also quantitatively. However, unfortunately it is a destructive modality; the sample should be dissected and carefully processed for imaging.

The OCT image was also taken using the same sample and shown in Fig. 4(f). As mentioned, the measurement was made from the side of the sample, i.e., from the top in Fig. 4(a). The figure clearly distinguishes the caries-involved region from the normal dentin region. The gully-like line at the caries area was curved. This curvature is believed to be due to rotation of the carries propagation along a fissure in the axial direction. We note that the imaging direction of OCT was different from the other four modalities; they were orthogonal to each other. As marked with the dotted circle in Fig. 4(f), the infected area gave a strong

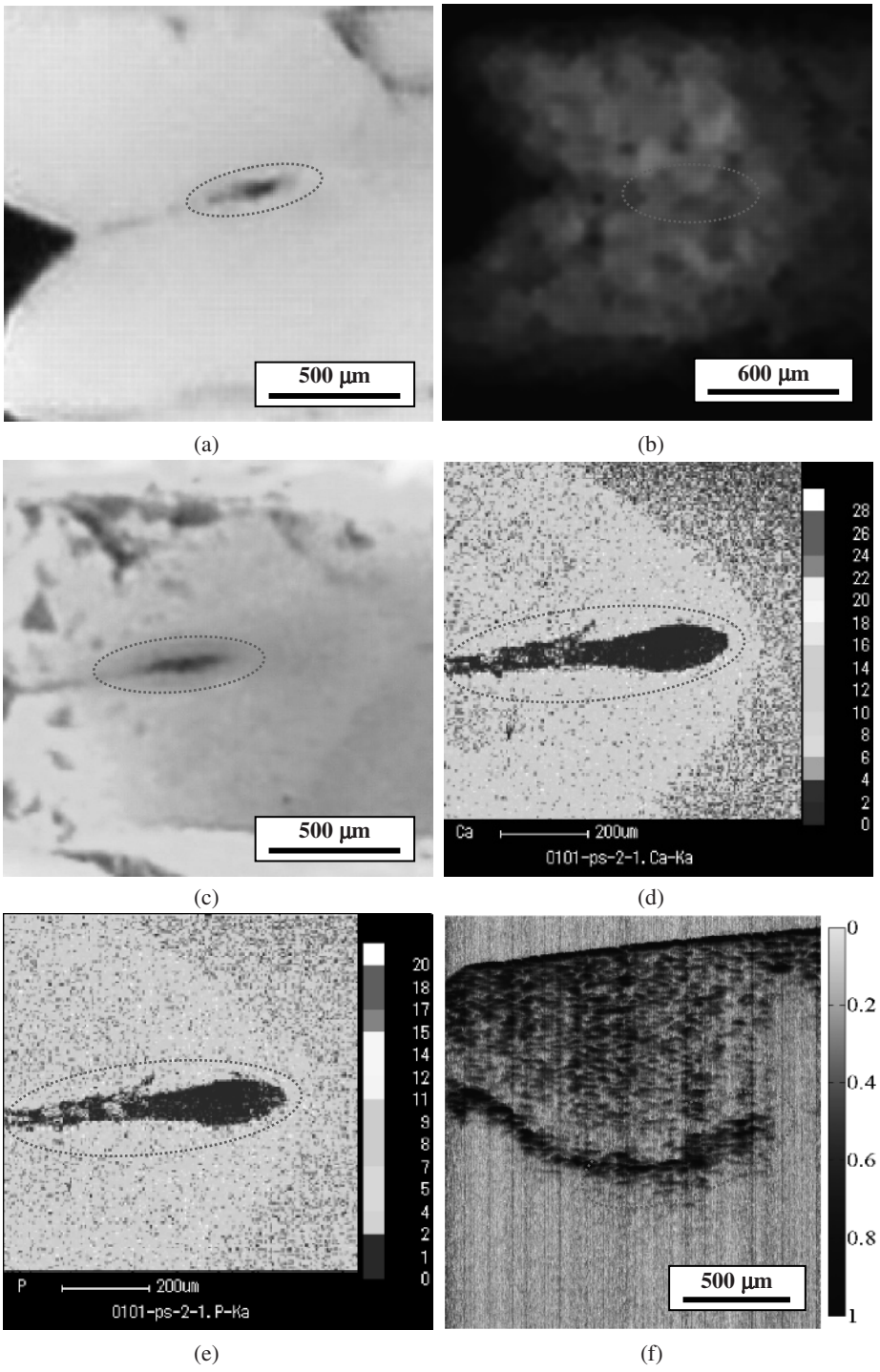

Fig. 4. (Color online) Images of the tooth sample (premolar, 32 male) obtained with different imaging tools. The dotted circle in each figure indicates the caries area; (a) photographic image; (b) DIOR image; (c) LIE image; (d) EPMA image of the calcium concentration; (e) EPMA image of the phosphate concentration; (f) OCT image.

OCT signal as the previous preliminary study shown with Fig. 2(c). By adopting PS-OCT[26] configuration, more detail information might be extracted through the polarization state change in the early caries lesion. Although the OCT image could not differentiate the chemical composition of the incipient caries as did EMPA images, it could clarify the position of the incipient caries without destroying the sample, unlike the other modalities.

Figure 5 shows some of the axial scan (A-scan) data sampled from the two-dimensional OCT image of Fig. 4(f). The dotted curve in the figure shows that the progressed caries lesion gives a strong OCT signal. We observed that the strongest reflected signal in the caries area happened at the transversal position of 0.84 mm. We believe that the destruction of the crystal-like structure and/or deficiency of calcium and phosphate caused by the caries greatly affected

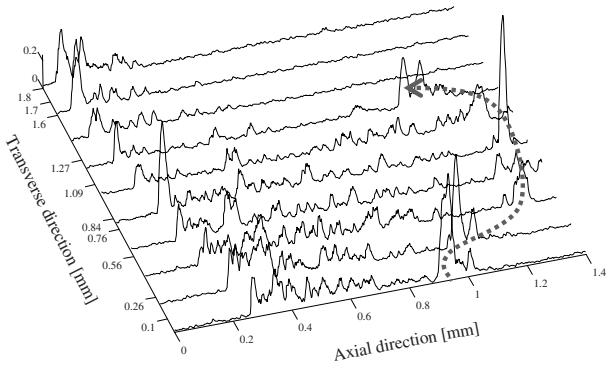

Fig. 5. (Color online) The axial scanning signals of Fig. 4(f) taken at the transverse positions of 0.1, 0.26, 0.56, 0.76, 0.84, 1.09, 1.27, 1.6, 1.7, and 1.8 mm, respectively. The strongest OCT signal was observed at the 0.84 mm transverse position and at the depth of 1.3 mm. The dotted curve indicates the propagation direction of the caries lesion.

the propagation of the OCT probing light. To get a more precise relationship among the modalities, more careful measurements with a well prepared sample are being readied. By utilizing full-field OCT, we can investigate the caries located near to the surface of a tooth with a very high lateral and depth resolution.[27)]

5. Conclusions

We have presented the OCT imaging modality used to diagnose dental caries in its incipient stage. With an extracted human tooth, the OCT image of the caries lesion was successfully obtained and compared with those taken with various modalities; EI, DIOR, LIE, and EPMA. Even by dissecting the sample to expose the infected region, DIOR could not distinguish the early caries lesion. EI, LIE, and EPMA could identify the caries, but the measurements were made destructively. However, OCT could non-invasively, and thus nondestructively, image the morphological feature of the dental structure with an axial resolution of $\sim$14 μm. Consequently, OCT might overcome the limitations of conventional dental diagnostics, especially in early caries, and thus be appropriate as an inspection tool in dentistry. By utilizing OCT, we could give patients objective diagnosis and conservative treatments in near future. In addition, safe diagnosis is possible with OCT even for radiation sensitive patient groups including pregnant women.

Acknowledgements

This work was supported in part by the Korea Science and Engineering Foundation (KOSEF) NCRC grant funded by the Korea government (MEST, No. R15-2008-006-02002-0), and by a grant from the Institute of Medical System Engineering (iMSE) in GIST, Korea.

References

1) W. G. Shafer, K. H. Maynard, and M. L. Barnet: *A Textbook of Oral Pathology* (W. B. Saunders, Philadelphia, PA, 1983) 4th ed., p. 406.
2) T. Koulourides: Proc. Symp. Incipient Caries of Enamel, University of Michigan School of Dentistry, 1977, p. 51.
3) T. Koulourides, H. Ceuto, and W. Pigman: Nature **189** (1961) 226.
4) J. C. Muhler, G. K. Stookey, and D. Bixler: J. Dent. Child. **3** (1965) 154.
5) O. Backer-Dirks: J. Dent. Res. **45** (1966) 503.
6) L. M. Silverstone: Br. Dent. J. **120** (1966) 461.
7) S. J. Zeichner, U. E. Ruttimann, and R. L. Webber: Radiology **162** (1987) 691.
8) A. Peers, F. J. Hill, C. M. Mitropoulos, and P. J. Holloway: Caries Res. **27** (1993) 307.
9) S. J. B. Reed: *Electron Microprobe Analysis* (Cambridge University Press, Cambridge, U.K., 2006) 2nd ed.
10) D. Huang, E. A. Swanson, C. P. Lin, J. S. Schuman, W. G. Stinson, W. Chang, M. R. Hee, T. Flotte, K. Gregory, C. A. Puliafito, and J. G. Fujimoto: Science **254** (1991) 1178.
11) W. Drexler: J. Biomed. Opt. **9** (2004) 47.
12) A. F. Fercher, C. K. Hitzenberger, G. Kamp, and S. Y. Elzaiat: Opt. Commun. **117** (1995) 43.
13) G. Hausler and M. W. Linduer: J. Biomed. Opt. **3** (1998) 21.
14) M. Wojtkowski, V. J. Srinivasan, T. H. Ko, A. Kowalczyk, J. S. Duker, and J. G. Fujimoto: Opt. Express **12** (2004) 2404.
15) B. W. Colston, Jr., U. S. Sathyam, L. B. DaSilva, M. J. Everett, P. Stroeve, and L. L. Otis: Opt. Express **3** (1998) 230.
16) F. I. Feldchtein, G. V. Gelikonov, V. M. Gelikonov, R. R. Iksanov, R. V. Kuranov, A. M. Sergeev, N. D. Gladkova, M. N. Ourutina, J. A. Warren, Jr., and D. H. Reitze: Opt. Express **3** (1998) 239.
17) B. T. Amaechi, S. M. Higham, A. Gh. Podoleanu, J. A. Rogers, and D. A. Jackson: J. Oral Rehabil. **28** (2001) 1092.
18) X. J. Wang, T. E. Milner, J. F. de Boer, Y. Zhang, D. H. Pashley, and J. S. Nelson: Appl. Opt. **38** (1999) 2092.
19) D. Fried, J. Xie, S. Shafi, J. D. B. Featherstone, T. M. Breuning, and C. Le: J. Biomed. Opt. **7** (2002) 618.
20) R. Brandenburg, B. Haller, and C. Hauger: Opt. Commun. **227** (2003) 203.
21) B. B. C. Kyotoku and A. S. L. Gomes: Opt. Commun. **279** (2007) 403.
22) A. Kunzel, D. Scherkowski, R. Willers, and J. Becker: Dentomaxillofac Radiol. **32** (2003) 385.
23) A. G. Farman and T. T. Farman: Oral Surg. Oral Med. Pathol. Oral Radiol. Endod. **99** (2005) 485.
24) A. M. Rollins, M. D. Kulkarni, S. Yazdanfar, R. Ungarunyawee, and J. Izatt: Opt. Express **3** (1998) 219.
25) C. C. Rosa and A. Gh. Podoleanu: Appl. Opt. **43** (2004) 4802.
26) S. Makita, Y. Yasuno, T. Endo, M. Itoh, and T. Yatagai: Opt. Rev. **12** (2005) 146.
27) W. J. Choi, J. Na, S. Y. Ryu, and B. H. Lee: J. Opt. Soc. Korea **11** (2007) 18.